Theory of surface polaritons in a polar zero-gap semiconductor

B. G. Martin and J. G. Broerman
McDonnell Douglas Research Laboratories, St. Louis, Missouri 63166
(Received 24 February 1981)

We have investigated the effect on surface polaritons of the $\Gamma_8^c \rightleftarrows \Gamma_8^v$ interband excitations of a polar α-Sn—type semiconductor, using HgTe as an example material. This case is of interest because, for certain ranges of impurity concentration, the optical-phonon surface polariton lies in the continuum of interband excitations, giving rise to the possibility of new surface-polariton modes. We find that in the zero-temperature, infinite-carrier-lifetime limit, a new mixed optical-phonon—interband-excitation mode does appear. For experimentally realizable temperatures and values of lifetime broadening, however, this mixed mode will likely not be observable. We find that the principal deviation from normal semiconductor behavior is a very tight binding of the longitudinal optical-phonon mode to the light line with corresponding long decay lengths.

I. INTRODUCTION

The fundamental energy gap of an α-Sn—type material (α-Sn, HgTe, HgSe, Cd_3As_2) is identically zero by reasons of symmetry.[1] The interband excitations possible in this unusual band structure lead to well-known anomalies[2] in the dielectric,[3–9] optical,[9,10] and transport[6,8,11–13] properties. In this paper, we investigate the effect of the zero-gap band structure on surface polaritons.

Figure 1 shows a schematic representation of the band structure near the zone center at absolute zero with impurity carriers present. In the absence of impurity carriers, the zero-energy excitation possible between the Γ_8 valence and conduction bands leads to a $\omega^{-1/2}$ singularity[3,4] in the frequency dependence and a q^{-1} singularity[5] in the momentum-transfer dependence of the dielectric response. As impurity carriers are added, the zero-energy excitation is no longer possible. However, because the joint density of available states as a function of excitation energy is now discontinuous, there will be a singularity (now logarithmic)[9] at a frequency corresponding to excitation to the Fermi energy. This frequency is continuously adjustable by varying the impurity carrier density.[9]

The dispersion relation for surface polaritons in a dielectrically isotropic medium is[14]

$$\frac{c^2k^2}{\omega^2} = \frac{\epsilon(\omega)}{\epsilon(\omega)+1} \quad . \tag{1.1}$$

In the absence of damping, i.e., when $\epsilon(\omega)$ is real, the asymptotic frequencies of the surface-polariton branches are given by the zeros of $\epsilon(\omega)+1$, leading in a normal polar semiconductor to plasmon polaritons and optical-phonon polaritons.

Thus, there is in the polar zero-gap semiconductor the possibility of additional surface-polariton branches arising from the interaction of the interband excitations and the optical phonons. In the frequency range between the transverse and longitu-

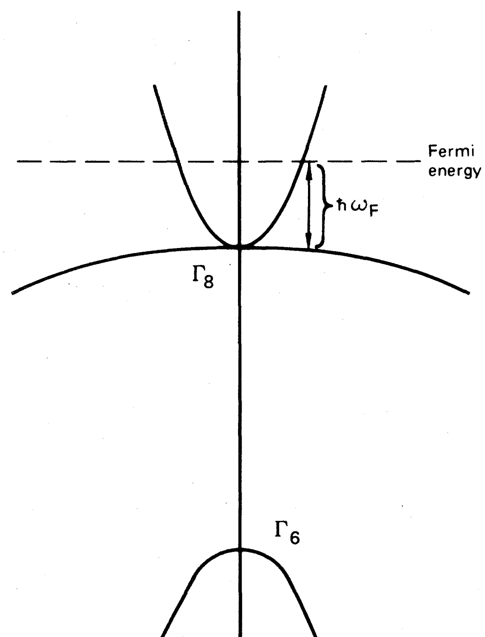

FIG. 1. Band structure of an α-Sn—type semiconductor.

dinal optical phonons, the dielectric function, excluding the contribution from the $\Gamma_8^c \rightleftarrows \Gamma_8^v$ interband excitation, is negative. If the carrier concentration is adjusted so that the excitation to the Fermi energy lies in this frequency range, two new zeros of $\epsilon(\omega)+1$ appear as a result of the singularity at the excitation threshold. These new zeros lead to the possibility of additional polariton branches. Furthermore, one would expect the polariton dispersion and decay parameters to differ significantly from those of a normal polar semiconductor because of the large imaginary component of the dielectric function associated with the $\Gamma_8^c \rightleftarrows \Gamma_8^v$ excitations.

However, the argument concerning the existence of new modes requires modification when we consider finite temperatures and lifetime broadening. For nonzero temperature and finite-carrier lifetime, $\epsilon(\omega)$ is nonsingular at, and its imaginary part is nonzero below, the excitation threshold.[9] The height and sharpness of the remanent peak at the excitation threshold, and hence the appearance of new polariton branches, depend on the numerical values of temperature and carrier lifetimes.

In what follows, we investigate surface polaritons in polar zero-gap semiconductors in detail, using HgTe as the example material. In Sec. II, the general surface-polariton dispersion relation for a polar zero-gap semiconductor is formulated. In Sec. III, the zero-temperature, infinite-lifetime limit is investigated, and in Sec. IV, the realistic nonzero-temperature, finite-lifetime case is examined.

II. DIELECTRIC FUNCTION AND SURFACE-POLARITON DISPERSION RELATION

We write the dielectric function in the form

$$\epsilon(\omega)=\epsilon^{\text{lat}}(\omega)+\epsilon^{\text{el}}(\omega) \ , \tag{2.1}$$

where ϵ^{lat} and ϵ^{el} are the lattice and electronic contributions, respectively. For the lattice part we use the usual phenomenological expression,

$$\epsilon^{\text{lat}}(\omega)=\frac{F\omega_{\text{TO}}^2}{\omega_{\text{TO}}^2-\omega^2+i\omega\Gamma} \ , \tag{2.2}$$

where

$$F=\frac{4\pi N e_T^{*2}}{\overline{M}\,\omega_{\text{TO}}^2} \ . \tag{2.3}$$

The quantity ω_{TO} is the transverse optical (TO) phonon frequency, e_T^* is the transverse effective charge, $\overline{M}$ is the unit-cell reduced mass, N is the number of unit cells per unit volume, and Γ is a reciprocal lifetime (or broadening) parameter. The electronic part is written as a sum of inter- and intraband (plasma) contributions,

$$\epsilon^{\text{el}}(\omega)=\epsilon^{\text{intra}}(\omega)+\epsilon^{\text{inter}}(\omega) \ , \tag{2.4}$$

where

$$\epsilon^{\text{intra}}(\omega)=-\frac{4\pi e^2}{m_0}\sum_j\frac{n_j}{\mu_j}\frac{1}{\omega^2+\tau_j^{-2}}\left[1-\frac{i}{\omega\tau_j}\right] \ , \tag{2.5}$$

and n_j, μ_j, and τ_j are, respectively, the number density, effective-mass ratio, and intraband lifetime of the jth-type of carrier. We have here, and in the following, assumed parabolic bands, an accurate approximation for $E_F << E_{\Gamma_8}-E_{\Gamma_6}$, which is satisfied for the range of carrier concentration of interest here.

The interband part is divided into the contribution from $\Gamma_8^v \leftrightarrows \Gamma_8^c$ excitations ϵ^{Γ_8} and a background part ϵ_b arising from all other excitations:

$$\epsilon^{\text{inter}}(\omega)=\epsilon_b+\epsilon^{\Gamma_8}(\omega) \ . \tag{2.6}$$

The background part ϵ_b is real and independent of frequency in the range of interest. The general form of ϵ^{Γ_8} is[9]

$$\epsilon^{\Gamma_8}(\omega)=\frac{2e^2}{\pi\hbar}\frac{(\mu_c m_0)^{1/2}}{1+\gamma}\frac{1}{(k_B T)^{1/2}}J(\omega) \ , \tag{2.7}$$

where

$$J(\omega)=\int_0^\infty\frac{G(y,z,\gamma)}{y^{1/2}}\left[\frac{1}{y-x-ix_I}+\frac{1}{y+x+ix_I}\right]dy \ , \tag{2.8}$$

$$G(y,z,\gamma)=\frac{\{1-\exp[-(1+\gamma)y]\}\exp(y-z)}{[1+\exp(-\gamma y-z)][1+\exp(y-z)]} \ , \tag{2.9}$$

$$x_I=T_I/[(1+\gamma)T]=\hbar/[k_B\tau_I(1+\gamma)T] \ , \tag{2.10}$$

$$x = \hbar\omega/[(1+\gamma)k_B T] \ , \tag{2.11}$$

$$\gamma = \mu_c/\mu_v \ , \tag{2.12}$$

and

$$z = E_F/k_B T \ . \tag{2.13}$$

Here τ_I is an interband lifetime and μ_c and μ_v are the conduction- and valence-band effective-mass ratios, respectively. The Fermi energy E_F is found from a numerical solution of the charge neutrality equation,

$$\frac{1}{2\pi^2}\left[\frac{2\mu_c m_0 k_B T}{\hbar^2}\right]^{3/2} \times [F_{1/2}(z) - \gamma^{-3/2}F_{1/2}(-z)] = n \ , \tag{2.14}$$

where $F_{1/2}(z)$ is the Fermi function of order $\frac{1}{2}$ and n is the donor density.

In solving the surface-polariton dispersion relation, Eq. (1.1), we take ω real and k complex, i.e.,

$$k = k_1 + ik_2 \ . \tag{2.15}$$

The surface-polariton decay length in the surface plane is $L = 1/(2k_2)$, and the surface-polariton decay constant into the bulk, α, is given by

$$\alpha^2 = k^2 - \frac{\omega^2}{c^2}\epsilon(\omega) > 0 \ . \tag{2.16}$$

The required HgTe parameters (at low temperature) are $\mu_c = 0.029$, $\mu_v = 0.53$, $\epsilon_b = 10.4$, $\omega_{TO} = 2.204 \times 10^{13}\ \mathrm{s}^{-1}$, and $F = 4.7$, as given by Grynberg *et al.*[10] The phonon reciprocal lifetime Γ varies from sample to sample, and we use[10] $\Gamma = 3.77 \times 10^{11}\ \mathrm{s}^{-1}$ as a characteristic value for the finite temperature and lifetime calculations presented in Sec. IV.

III. ZERO-TEMPERATURE INFINITE-LIFETIME LIMIT

For the case of $T \to 0$ and $\tau_I \to \infty$, the general expression for the $\Gamma_8^c \rightleftarrows \Gamma_8^v$ contribution to the dielectric function reduces to the simple form[9]

$$\epsilon^{\Gamma_8}(\omega) = \frac{2\sqrt{2}e^2}{\pi\hbar^{3/2}}\left[\frac{\mu_c m_0}{1+\gamma}\right]^{1/2}\frac{1}{\omega^{1/2}}\left\{\frac{\pi}{2} - \tan^{-1}\left[\left[\frac{\omega_F}{\omega}\right]^{1/2}\right] + \tfrac{1}{2}\ln\left|\frac{1+(\omega_F/\omega)^{1/2}}{1-(\omega_F/\omega)^{1/2}}\right| + i\frac{\pi}{2}\Theta(\omega-\omega_F)\right\} , \tag{3.1}$$

where ω_F is the frequency threshold for excitation to the Fermi energy and is given by

$$\omega_F = \frac{(1+\gamma)E_F}{\hbar} \ . \tag{3.2}$$

In Eq. (3.1), $\Theta(x)$ is a step function which is 0 for $x < 0$ and 1 for $x \geq 0$. Since the carrier distribution is degenerate, E_F is given by

$$E_F = \frac{\hbar^2}{2\mu_c m_0}(3\pi^2 n)^{2/3} \ . \tag{3.3}$$

For this idealized situation, we also take the phonon damping Γ to be zero. The various contributions to $\epsilon(\omega)$ vs ω are shown in Fig. 2 for $n = 3.9 \times 10^{16}\ \mathrm{cm}^{-3}$. As pointed out in the Introduction, the real part of $\epsilon(\omega)$ has a singularity at $\omega = \omega_F$, and, even for infinite electron and phonon lifetimes, the interband excitations provide a large imaginary part for $\epsilon(\omega)$ for $\omega \geq \omega_F$.

In a normal finite-gap polar semiconductor with no damping and a plasma frequency ω_p less than the transverse optical-phonon frequency ω_{TO}, the surface polaritons exhibit a plasmonlike mode, which begins at zero frequency and asymptotically approaches the bulk plasmon frequency, and a phononlike mode, which begins on the lightline at ω_{TO} and asymptotically approaches the surface LO phonon polariton frequency ω_{LO}. Both of these modes lie to the right of the lightline.

For the zero-gap semiconductor, the surface-polariton behavior is qualitatively different in three distinct ranges of ω_F (or alternatively, of carrier concentration). These ranges are $\omega_F < \omega_{TO}$, $\omega_{TO} \leq \omega_F < \omega_{LO}$, and $\omega_F > \omega_{LO}$.

A. $\omega_F < \omega_{TO}$

The surface-polariton dispersion for HgTe for $\omega_F = 0.42\omega_{TO}$ ($n = 10^{16}\ \mathrm{cm}^{-3}$) is shown in Fig. 3. The lowest lying polariton branch is the normal

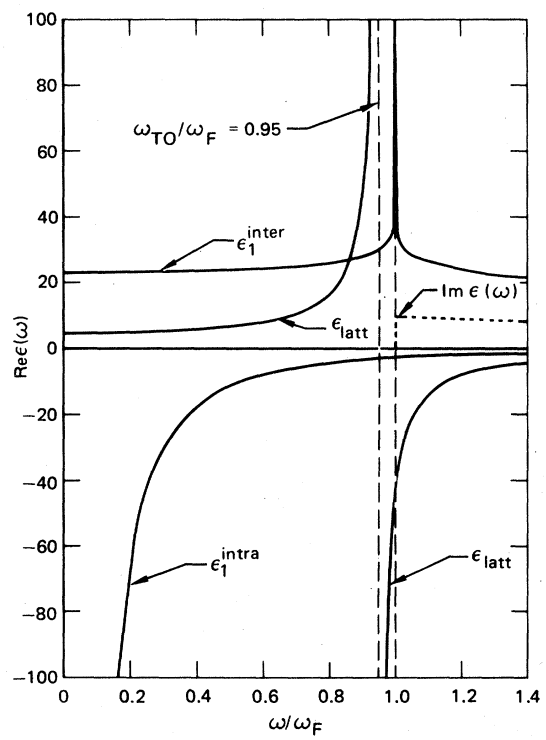

FIG. 2. Dielectric function of HgTe in the zero-temperature, infinite-carrier-lifetime limit for $n = 3.9 \times 10^{16}\ \mathrm{cm}^{-3}$.

plasmonlike mode. The only effect of the interband excitations on this mode is to depress it more strongly with decreasing carrier concentration than in a normal semiconductor because of the increase in $\epsilon^{\Gamma_8}(\omega)$ with decreasing n_e.

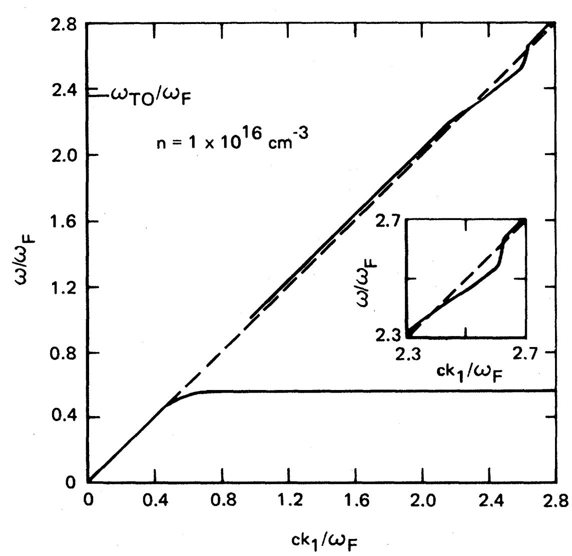

FIG. 3. Surface-polariton dispersion in HgTe in the degenerate infinite-lifetime limit ($\omega_F/\omega_{\mathrm{TO}} = 0.424$)

A second branch, a Zenneck mode[15] lying to the left of the light line, begins at $\omega = \omega_F$. This mode moves upward with frequency, crosses the light line at ω_{TO}, and subsequently recrosses the light line to the left at approximately the bulk LO phonon frequency. The backbending behavior for $\omega \geq \omega_{\mathrm{TO}}$ is a result of the phonons lying in the continuum of interband excitations and therefore in a frequency range with a large $\mathrm{Im}\epsilon(\omega)$. This behavior, except for the gap between ω_p and ω_{TO}, is reminiscent of the surface-polariton behavior in a highly damped, normal polar semiconductor, where the nonzero $\mathrm{Im}\epsilon(\omega)$ is produced by intraband excitations.

The frequency dependence of the imaginary part of the polariton wave vector is shown in Fig. 4. At $\omega = \omega_F$, k_2 increases rapidly to a large value, reflecting the onset of the interband excitations, and then with increasing frequency, rapidly decreases to zero at $\omega = \omega_{\mathrm{TO}}$ because of the singularity in $\epsilon(\omega)$ at that frequency. For frequencies above ω_{TO}, k_2 again increases rapidly with frequency. The behavior of k_2 for the optical-phonon-like modes, $\omega \gtrsim \omega_{\mathrm{TO}}$, is again typical of that in a highly damped, normal polar semiconductor.

B. $\omega_{\mathrm{TO}} \leq \omega_F < \omega_{\mathrm{LO}}$

In what follows, ω_{LO} is taken to be the highest lying zero of $\epsilon(\omega) + 1$. This value is consistent for our purpose since the mode structure changes discontinuously at $\omega_F = \omega_{\mathrm{LO}}$ when ω_{LO} is defined in this way. In HgTe, the approximate range of carrier concentration corresponding to $\omega_{\mathrm{TO}} \leq \omega_F < \omega_{\mathrm{LO}}$ is $3.62 \times 10^{16} \leq n \leq 4.03 \times 10^{16}$.

The surface-polariton dispersion in HgTe is shown in Fig. 5 for $\omega_F/\omega_{\mathrm{TO}} = 1.05$ ($n = 3.9 \times 10^{16}$

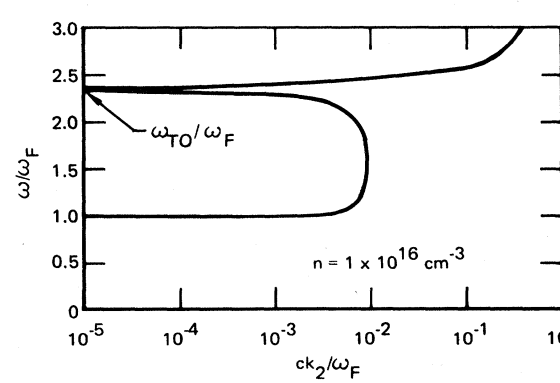

FIG. 4. Frequency dependence of the imaginary part of the wave vector associated with surface polaritons in HgTe in the degenerate infinite-lifetime limit ($\omega_F/\omega_{\mathrm{TO}} = 0.424$).

cm^{-3}). The lowest lying plasmonlike mode is qualitatively the same as that of a normal semiconductor. The next higher polariton mode begins on the light line at $\omega = \omega_{TO}$, increases with frequency, and asymptotically approaches the zero of $1 + \epsilon(\omega)$ slightly below ω_F. The final mode, which lies in the continuum of interband excitations, begins on the light line at ω_F, increases with frequency, and then backbends because of the presence of $\mathrm{Im}\epsilon(\omega)$ in this frequency range, crossing the light line at $\omega \approx \omega_{LO}$. It then continues with increasing frequency as a Zenneck mode almost parallel to the light line. These last two modes are surface polaritons associated with optical-phonon—interband-excitation interaction, and their behavior is qualitatively different from that of a normal, undamped polar semiconductor. In effect, for n_e in the range $3.62 \times 10^{16} \leq n \leq 4.03 \times 10^{16}$ cm^{-3}, the normal optical-phonon polariton mode is split into two parts by the mixing of the optical-phonon—interband transitions.

The frequency dependence of the imaginary part of the wave vector k_2 is shown in Fig. 6. Note that k_2 increases rapidly with frequency from zero to a maximum at $\omega = \omega_F$, the onset of the interband excitations, and then rapidly decreases to a minimum as $\mathrm{Re}\epsilon(\omega)$ goes through -1. This minimum is a remanent of the mode which would have an asymptotic frequency corresponding to this zero of $\epsilon(\omega) + 1$ if $\mathrm{Im}\epsilon(\omega)$ were zero. The value of k_2 again increases with frequency to another maximum as the corresponding polariton-dispersion mode (Fig. 5) backbends across the light line. Finally, k_2 slowly decreases with increasing frequency in the Zenneck region. Both the plasmon and TO-phonon—interband-excitation modes are undamped.

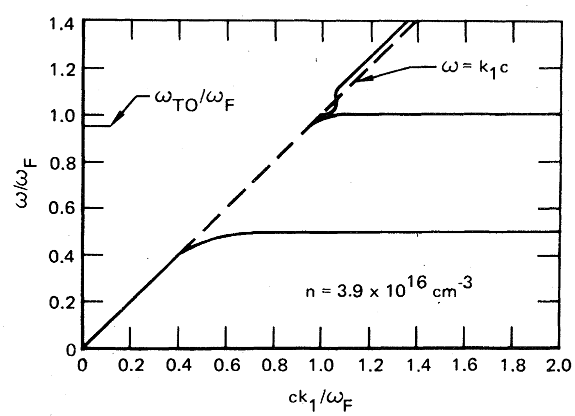

FIG. 5. Surface-polariton dispersion in HgTe in the degenerate infinite-lifetime limit ($\omega_F/\omega_{TO} = 1.053$).

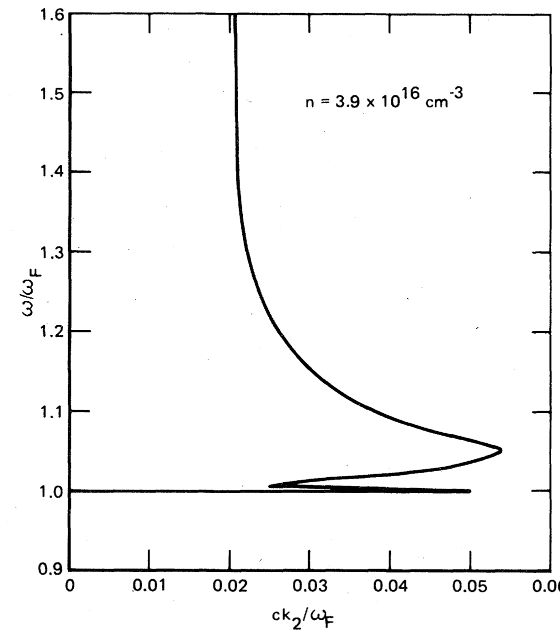

FIG. 6. Frequency dependence of the imaginary part of the wave vector associated with surface polaritons in HgTe in the degenerate infinite-lifetime limit ($\omega_F/\omega_{TO} = 1.053$).

C. $\omega_F > \omega_{LO}$

In this frequency range, the plasmon- and phononlike polaritons behave like those in a normal polar semiconductor. The surface-polariton dispersion is shown in Fig. 7 for $\omega_F/\omega_{TO} = 1.96$ ($n = 10^{17}$ cm^{-3}). The only feature unique to zero-gap semiconductors is the Zenneck mode (associated with the interband excitations) beginning at $\omega = \omega_F$ and increasing with increasing frequency. As the carrier concentration is increased further, interaction between the plasmon- and phononlike modes will begin eventually, and this interaction will not differ qualitatively from the like situation in a normal semiconductor. Figure 8 shows the corresponding frequency dependence of the imaginary part of the wave vector which begins at $\omega = \omega_F$ and increases with frequency.

IV. FINITE TEMPERATURE AND CARRIER LIFETIMES

As is evident from the preceding discussion, the case which can exhibit the new mixed mode structure is that of $\omega_{TO} \leq \omega_F \leq \omega_{LO}$. We now examine this case for finite temperature and carrier lifetimes, as well as finite-phonon damping.

We have been unable to find an experimental

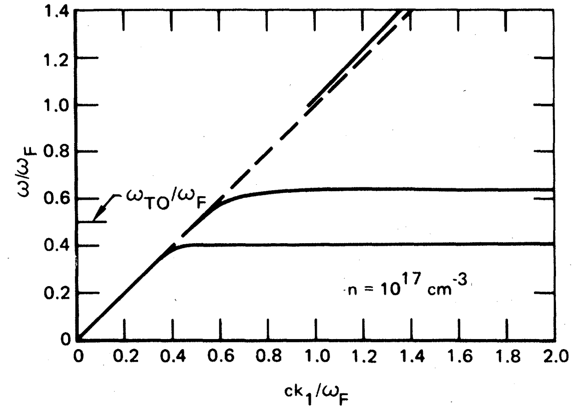

FIG. 7. Surface-polariton dispersion in HgTe in the degenerate infinite-lifetime limit ($\omega_F/\omega_{TO} = 1.961$).

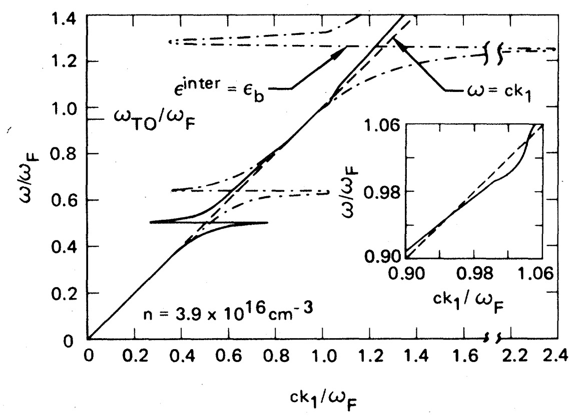

FIG. 9 Surface-polariton dispersion in HgTe at $T = T_I = 1$ K ($\omega_F/\omega_{TO} = 1.053$, $\Gamma = 3.77 \times 10^{11}$ s^{-1}).

determination of τ_I for HgTe. However, in small-gap $Hg_{1-x}Cd_xSe$ alloys,[16] $T_I = 1$ K is typical of so-called "good" samples at liquid-helium temperatures, and we adopt this value. Because the dielectric function near the degenerate singularity changes little[9] for T below T_I, we also choose $T = 1$ K, which is also probably the lower limit for achievable experimental temperatures in, for example, an attenuated total reflection[17] experiment. Finally, we use interband lifetimes ($\hbar/\tau_i = k_B T_i$) corresponding to $T_i = 1$ K, and the phonon reciprocal lifetime $\Gamma = 3.77 \times 10^{11}$ s^{-1}.

The surface-polariton dispersion for this situation and $n = 3.9 \times 10^{16}$ cm^{-3} (the same as in Fig. 7 except for nonzero T, finite lifetimes, and phonon damping) is given by the solid curve of Fig. 9. The dashed curve of Fig. 9 is for the same case except that the ϵ^{Γ_8} contribution is removed for comparison with a normal semiconductor. The upward shift of the dashed curve is because of removal of some of the contribution to $\mathrm{Re}\epsilon(\omega)$ and is of no importance. As can be seen, the two cases are qualitatively the same, except that the optical-phonon polariton mode is more tightly bound to the light line in the zero-gap case (the inset of Fig. 9 shows a magnification of this region). The reason for this tightly bound mode behavior is the large value of $\mathrm{Im}\epsilon(\omega)$ produced by the interband excitations.

For the values of T_I and T used here, $\mathrm{Re}\epsilon(\omega = \omega_F)$ is less than -1, and there is no evidence in Fig. 9 of the TO-phonon—interband-excitation branch that appears in Fig. 5 for the degenerate, infinite-lifetime case. For the values $T_I = T = 1$ K, this is true for all carrier concentrations. One would have to reduce both T and T_I by at least 2 orders of magnitude for any effect in the dispersion related to the TO-phonon—interband-excitation branch to appear.

The frequency dependence of the imaginary part of the wave vector k_2 is shown in Fig. 10. For fre-

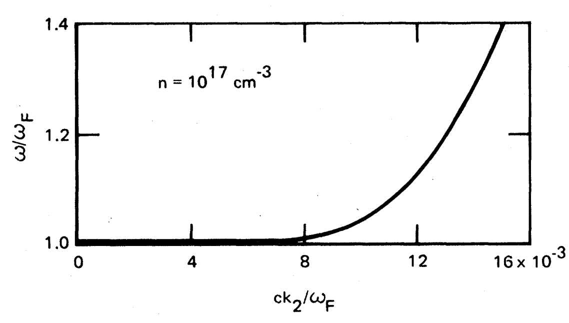

FIG. 8. Frequency dependence of the imaginary part of the wave vector associated with surface polaritons in HgTe in the degenerate infinite-lifetime limit ($\omega_F/\omega_{TO} = 1.961$).

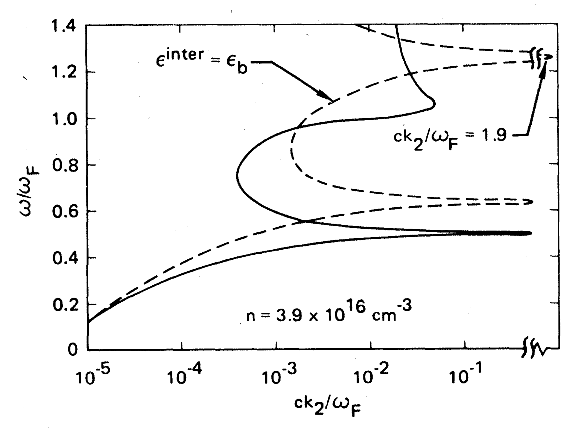

FIG. 10. Frequency dependence of the imaginary part of the wave vector associated with surface polaritons in HgTe at $T = T_I = 1$ k ($\omega_F/\omega_{TO} = 1.053$, $\Gamma = 3.77 \times 10^{11}$ s^{-1}).

quencies of the plasmonlike polariton, the behavior of k_2 is qualitatively the same as that for normal semiconductors. However, in the frequency region of the optical-phonon polariton, the interband excitations produce a considerable reduction in the attenuation. This follows from the fact that in the neighborhood of the backbending across the light line,

$$k_2 \approx \frac{\omega}{2c} \frac{1}{\mathrm{Im}\epsilon(\omega)} \quad . \tag{4.1}$$

Thus, since the interband excitations at frequencies above ω_F produce a much larger value for $\mathrm{Im}\epsilon(\omega)$ than the intraband excitations, which are the only source of damping in normal semiconductors, one would expect the surface polariton in a zero-gap semiconductor to be considerably less attenuated at frequencies around ω_{LO} for $\omega_F < \omega_{\mathrm{LO}}$ than in normal semiconductors.

V. SUMMARY

In the degenerate, infinite-carrier-lifetime limit, there are distinct qualitative differences in surface-polariton dispersion between a zero-gap and normal semiconductor, the most important of which involves mixing of optical-phonon-like and interband-excitation-like modes. However, in a realistic situation, this new mode structure will probably not be observable because of temperature and lifetime broadening. The singularity associated with the discontinuity in the degenerate joint available density of states in the doped zero-gap band structure is a narrow logarithmic divergence and therefore requires only a small temperature broadening of the electron-distribution function or lifetime broadening of the energy levels to reduce the remanent peak to a point where its effect on surface-polariton dispersion is insufficient to produce the new mode structure.

However, the quantitative differences from a normal semiconductor are substantial. The interband excitations above the Fermi frequency produce considerably tighter binding of the surface-polariton dispersion to the light line, as well as considerably less attenuation than expected in a comparable normal semiconductor. These effects may be observable experimentally by attenuated total reflection.[17]

ACKNOWLEDGMENT

This research was conducted under the McDonnell Douglas Independent Research and Development program.

[1] S. Groves and W. Paul, Phys. Rev. Lett 11, 194 (1963).
[2] For a review, see J. G. Broerman, in *Proceedings of the Eleventh International Conference on the Physics of Semiconductors,* edited by M. Miasek (PWN- Polish Scientific, Warsaw, 1972), p. 918.
[3] D. Sherrington and W. Kohn, Rev. Mod. Phys. 40, 767 (1968).
[4] B. I. Halperin and T. M. Rice, Rev. Mod. Phys. 40, 756 (1968).
[5] L. Liu and D. Brust, Phys. Rev. Lett. 20, 651 (1968).
[6] L. Liu and E. Tosatti, Phys. Rev. Lett. 23, 772 (1969).
[7] J. G. Broerman, Phys. Rev. Lett. 25, 1658 (1970).
[8] J. G. Broerman, L. Liu, and K. N. Pathak, Phys. Rev. B 4, 664 (1971).
[9] J. G. Broerman, Phys. Rev. B 5, 397 (1972).
[10] M. Grynberg, R. LeToulec, and M. Balkanski, Phys. Rev. B 9, 517 (1974).
[11] J. G. Broerman, Phys. Rev. Lett. 24, 450 (1970); Phys. Rev. B 1, 4568 (1970); 2, 1818 (1970).
[12] J. G. Broerman, J. Phys. Chem. Solids 32, 1263 (1971).
[13] S. L. Lehoczky, J. G. Broerman, D. A. Nelson, and C. R. Whitsett, Phys. Rev. B 9, 1598 (1974).
[14] *Polaritons, Proceedings of the First Taormina Research Conference on the structure of Matter, Taormina, Italy, 1972,* edited by Elias Burstein and Francesco de Martini (Pergamon, New York, 1974).
[15] H. Wolter in *Handbuch der Physik,* edited by S. Flügge (Springer, Berlin, 1965), Bd. xxiv, p. 474.
[16] C. J. Summers and J. G. Broerman, Phys, Rev. B 21, 559 (1980).
[17] A. Otto, Z. Phys. 216, 398 (1968).